2-14-2017

Brownian motion of solitons in a Bose-Einstein Condensate

Lauren M. Aycock
University of Maryland

Hilary M. Hurst
University of Maryland, hilary.hurst@sjsu.edu

Dimitry K. Efimkin
University of Texas at Austin

Dina Genkina
University of Maryland

Hsin-I Lu
University of Maryland

See next page for additional authors

Recommended Citation

Lauren M. Aycock, Hilary M. Hurst, Dimitry K. Efimkin, Dina Genkina, Hsin-I Lu, Victor M. Galitski, and I. B. Spielman. "Brownian motion of solitons in a Bose-Einstein Condensate" *Proceedings of the National Academy of Sciences* (2017). https://doi.org/10.1073/pnas.1615004114

Impurity driven Brownian motion of solitons in elongated Bose-Einstein Condensates

L. M. Aycock[1,2], H. M. Hurst[1,3], D. Genkina[1], H.-I Lu[1], V. Galitski[1,3], I. B. Spielman[1]

[1]*Joint Quantum Institute, National Institute of Standards and Technology, and University of Maryland, Gaithersburg, Maryland, 20899, USA*

[2]*Cornell University, Ithaca, New York, 14850, USA*

[3]*Condensed Matter Theory Center, Department of Physics, University of Maryland, College Park, Maryland 20742, USA*

Solitons, spatially-localized, mobile excitations resulting from an interplay between nonlinearity and dispersion, are ubiquitous in physical systems from water channels[1] and oceans[2] to optical fibers[3] and Bose-Einstein condensates (BECs)[4]. For the first time, we observed and controlled the Brownian motion[5] of solitons. We launched long-lived dark solitons in highly elongated ^{87}Rb BECs and showed that a dilute background of impurity atoms in a different internal state dramatically affects the soliton. With no impurities and in one-dimension (1-D), these solitons would have an infinite lifetime, a consequence of integrability. In our experiment, the added impurities scatter off the much larger soliton, contributing to its Brownian motion and decreasing its lifetime. We describe the soliton's diffusive behavior using a quasi-

1-D scattering theory of impurity atoms interacting with a soliton, giving diffusion coefficients consistent with experiment.

From our pulse throbbing at our wrists to rapidly moving tsunamis, solitons appear naturally at a wide range of scales[6]. In non-linear optical fibers, solitons can travel long distances with applications to communication technology and potential for use in quantum switches and logic[3,7]. Understanding how random processes contribute to the decay and the diffusion of solitons is essential to advancing these technologies. We studied this physics in the highly controlled quantum environment provided by atomic Bose-Einstein condensates (BECs), where density maxima can be stabilized by attractive interactions, i.e., bright solitons[8]; or as here, where density depletions can be stabilized by repulsive interactions, i.e., dark solitons[4,9]. By contaminating these BECs with small concentrations of impurity atoms, we quantitatively studied how random processes destabilize solitons.

Our BECs can be modeled by the one-dimensional (1-D) Gross-Pitaevski equation (GPE): an integrable nonlinear wave equation with soliton solutions as excitations above the ground state. For a homogeneous 1-D BEC of particles with mass m_{Rb} with density ρ_0, speed of sound c, and healing length $\xi = \hbar/\sqrt{2m_{\mathrm{Rb}}c}$, the dark soliton solutions

$$\varphi(z,t) = \sqrt{\rho_0}\left[i\frac{v_s}{c} + \frac{\xi}{\xi_s}\tanh\left(\frac{z-v_s t}{\sqrt{2}\xi_s}\right)\right] \tag{1}$$

are expressed in terms of time t, axial position z, soliton velocity v_s, and soliton width $\xi_s =$

$\xi/\sqrt{1-(v_s/c)^2}$. Such dark solitons have a minimum density $\rho_0(v_s/c)^2$ and a phase jump $-2\cos^{-1}(v_s/c)$ both dependent upon the soliton velocity v_s. These behave as classical objects with a negative inertial mass m_s, essentially the missing mass of the displaced atoms. The negative mass implies that increasing the velocity reduces the kinetic energy, thus dissipation accelerates dark solitons[10]. This can be seen from the soliton equation of motion

$$m_s\ddot{z}(t) = -\gamma\dot{z}(t) - \partial_z V + f(t), \tag{2}$$

where V is the axial confining potential and $-\gamma\dot{z}$ is the friction force. The random Langevin force $f(t)$ has a white noise correlator $\langle f(t)f(t')\rangle = 2\gamma k_{\rm B}T\delta(t-t')$ for temperature T and Boltzmann constant $k_{\rm B}$. The friction coefficient $\gamma = D/k_{\rm B}T$ is related to the diffusion coefficient D describing friction from the impurity atoms. The connection between γ and $f(t)$ is a manifestation of the fluctuation-dissipation theorem - $f(t)$ is responsible for Brownian motion while γ describes friction, but both have contributions from impurity atoms.

Idealized solitons are infinitely long-lived due to the integrability of the 1-D GPE. Integrability breaking is inherent in all physical systems, for example from the non-zero transverse extent of quasi-1-D systems. Indeed in experiments, solitons are only long-lived in highly elongated geometries[11–13], where integrability breaking is weak. Cold atom experiments have profoundly advanced our understanding of soliton instability by controllably

lifting integrability by tuning the dimensionality[14,15]. Here, we studied the further lifting of integrability by coupling solitons to a reservoir of impurities.

Our system[16] consisted of an elongated $^{87}\mathrm{Rb}$ BEC, confined in a nominally flat-bottomed time-averaged potential, created by spatially dithering one beam of our crossed dipole trap. We prepared $N = 8(2) \times 10^5$ atoms[1] in the $|F = 1, m_F = 0\rangle$ internal state at $T = 10(5)$ nK. Our system's $\approx 250\ \mu\mathrm{m}$ longitudinal extent was about 30 times its transverse Thomas-Fermi diameter $2R_\perp$ set by the radial trap frequency $\omega_r = 2\pi \times 115(2)$ Hz and chemical potential $\mu \approx h \times 1$ kHz. We controllably introduced a uniform[17] gas of N_I impurity atoms in thermal equilibrium with our BECs using an rf pulse resonant with the $|F = 1, m_F = 0\rangle$ to $|F = 1, m_F = +1\rangle$ transition prior to evaporation to degeneracy[18]. This gave impurity fractions N_I/N from 0 to 0.062 in our final BECs. We then launched lone long-lived dark solitons using a phase imprinting technique[4,9].

We absorption-imaged our solitons after a sufficiently long time-of-flight (TOF) that their initial width $\xi_s \approx 0.24\ \mu\mathrm{m}$ expanded beyond our $\approx 2\ \mu\mathrm{m}$ imaging resolution. Figure 1**a** is an image of our elongated BEC with no soliton present, and in contrast Fig. 1**b** displays an image of a BEC with a dark soliton taken 0.947 s after its inception. The soliton is the easily identified density depletion sandwiched between two density enhancements. We quantitatively identified the soliton position as the minimum of the density depletion from

[1] In our system, number fluctuations increased at the lowest trap depth (see methods).

1-D distributions (right panel of Fig. 1 **b**). Our phase imprinting process launched several excitations in addition to the dark soliton of interest. After a few hundred milliseconds, the additional excitations dissipated and the remaining soliton was identified. By backtracking the soliton trajectory, we were able to distinguish the soliton even at short times.

Figure 1**c** shows a series of 1-D distributions taken from time $t \approx 0$ s to 4 s after the phase imprint. These images show three salient features: (1) the soliton underwent approximately sinusoidal oscillations, (2) the soliton was often absent at long times, and (3) there was significant scatter in the soliton position. Items (2) and (3) suggests that random processes were important to the soliton's behavior. The solitons' position z_i–when present–is represented by the light pink symbols in Fig. 1**d** and the darker pink symbols mark the average position $\langle z_i \rangle$ for each time t.

Having established a procedure for creating solitons, we turned to the impact of coupling to a reservoir of impurities, thus further breaking integrability. Figure 2 displays the soliton position versus time for a range of impurity fractions. Adding impurities gave two dominant effects[2]: further increasing the scatter in the soliton position z and further decreasing the soliton lifetime. These effects manifested as a reduced fraction f_s of images with a soliton present and an increase in the sample variance $\mathrm{Var}(z) = \sum (z_i - \langle z \rangle)^2 / (M-1)$

[2]The soliton oscillation frequency was slightly shifted with impurities resulting from an unintentional change in the underlying optical potential. This change also slightly reduced the BECs longitudinal extent.

computed using the number M of measured positions z_i at each time.

The addition of impurities had a dramatic impact on the soliton lifetime. While we lack a quantitative model of the soliton's decay mechanism, there are several reasons to expect a finite lifetime. When dissipation is present, solitons accelerate to the speed of sound and disintegrate. Additionally, because our trap geometry has a finite transverse extent, quantified by the ratio $\mu/\hbar\omega_r \approx 9$, solitons can be dynamically unstable and decay into 3-D excitations[19]. Our soliton's initial velocity $v_s \approx 0.3\ \mathrm{mm/s}$, roughly $1/5$ the 1-D speed of sound $c \approx 1.4\ \mathrm{mm/s}$[20], implies it is in an unstable regime, where, as observed, it should decay[10]. Furthermore, numerical simulations show that in anharmonic traps solitons lose energy by phonon emission, accelerate, and ultimately decay[21]. All of these decay mechanisms can contribute to the soliton lifetime even absent impurities.

The added impurities act as scatterers impinging on the soliton, further destabilizing it. This effect is captured in Fig. 3**a**, showing the measured survival probability f_s versus time for a range of impurity fractions. We fit to our data a model of the survival probability

$$f_s(t) = 1 - \frac{1}{2}\,\mathrm{erfc}\left[\frac{-\ln(t/\tau)}{\sqrt{2}\sigma}\right], \tag{3}$$

essentially the integrated lognormal distribution of decay times, suitable for decay due to accumulated random processes[22]. The survival probability $f_s(t)$ has a characteristic width parameterized by σ and reaches $1/2$ at time τ which we associate with the soliton

lifetime. Figure 3**b** shows the extracted lifetime τ versus impurity fraction $N_{\rm I}/N$, showing a monotonic decrease. Our maximum $N_{\rm I}/N$ gives a factor of four decrease in lifetime τ.

The second important consequence of adding impurities was an increased scatter in soliton position z, reminiscent of Brownian motion. Indeed, as shown in Fig. 4**a**, this scatter, quantified by $\mathrm{Var}(z)$, increased linearly with time. We obtained the diffusion coefficient D as the slope from linear fits to these data and calculated D using a quasi-1-D scattering theory. The energy of the infinitely long 1-D system is given by the GPE energy functional

$$E\left[\varphi,\psi\right]=\int dz\frac{\hbar^2}{2m_{\rm Rb}}|\nabla\varphi|^2+\frac{\hbar^2}{2m_{\rm Rb}}|\nabla\psi|^2+\frac{g}{2}|\varphi|^2|\varphi|^2+\frac{g'}{2}|\varphi|^2|\psi|^2, \tag{4}$$

describing the majority gas interacting with itself along with the impurities with interaction coefficients g and g', respectively. The fields φ and ψ denote the condensate and impurity wavefunctions. Since the impurities are very dilute, we do not include interactions between impurity atoms. A soliton [Eq. (1)] gives a supersymmetric Pöschl-Teller[23,24] potential for the impurity atoms with exact solutions in terms of hypergeometric functions[25]. Impurity scattering states with momentum k_z in the rest frame of the soliton are described by the reflection coefficient

$$R(k_z)=\frac{1-\cos(2\pi\lambda)}{\cosh(2\pi k_z\xi)-\cos(2\pi\lambda)}, \tag{5}$$

where $\lambda(\lambda-1)=g'/g$. In $^{87}\mathrm{Rb}$, we have $g\approx g'$, giving $\lambda\approx 1.5$. The scattering problem is fully characterized by $R(k_z)$ and the problem is reduced to that of a classical heavy

object moving through a gas of lighter particles.

We treat the soliton using Eq.(2) with the stochastic force due to elastic collisions with the impurity atoms. The collision integral can be expressed in Fokker-Planck form[26](see methods) with diffusion coefficient

$$D = \frac{(k_{\mathrm{B}}T)^2}{B}, \tag{6}$$

giving $Dt = \mathrm{Var}(x)$. Momentum diffusion is described by the transport coefficient

$$B = 2\hbar \sum_{m,l} \int_{-\infty}^{\infty} \frac{dk_z}{2\pi} k_z^2 \left| \frac{\partial \epsilon}{\partial k_z} \right| R(k_z) n(\epsilon) \left[1 + n(\epsilon)\right], \tag{7}$$

an extension of reference[27]. $\epsilon_{m,l}(k_z) = \hbar^2 k_z^2 / 2m_{\mathrm{Rb}} + \hbar^2 j_{m,l}^2 / 2m_{\mathrm{Rb}} R_\perp^2$ is the impurities' quasi-1D dispersion along with quantized states in the radial direction, described by Bessel functions. We account for radial confinement by summing over quantum numbers m and l. $n(\epsilon)$ is the Bose-Einstein distribution for impurity atoms[3].

Figure 4**b** plots D measured experimentally (markers) and computed theoretically (curves, colored for different temperatures) as a function of N_{I}/N. The parameter-free theory provides rather accurate estimets of the experimentally observed diffusion coefficient. Any additional scatterers would also contribute to the transport coefficient B, and since $D \propto 1/B$, the diffusion coefficient should be smaller for more scatterers. In our quasi-1-D system, the soliton is not reflectionless to phonons in the majority gas as in the true 1-D

[3]In our model, condensed atoms do not contribute to diffusion

problem, however we have not considered them and they can reduce D. Lastly, we note that at $N_I/N = 0$, D is suppressed, in contrast with the prediction of our theory. The precise mechanism of dissipation without impurities cannot be identified within the scope of our theory and the observation of reduced diffusion remains an outstanding problem.

Solitons in spinor systems with impurity scatterers is an exciting playground for studying integrability breaking and diffusion of quasi-classical, negative-mass objects. Our observed reduction in soliton lifetime with increasing impurity fraction is in need of a quantitative theory. For the case of no impurities there is a further open question for both theory and experiment of whether friction and diffusion can be present even in the case of preserved integrability, for example due to non-Markovian effects, as was recently discovered for bright solitons [28]. Future experiments could study the impact of different types of impurities on soliton dynamics by introducing impurities of a different atomic mass. Lastly, mixtures with tunable interactions could freely tune the amount of integrability breaking.

Methods

BEC creation. We created BECs in the optical potential formed by a pair of crossed horizontal laser beams of wavelength $\lambda = 1064\,\mathrm{nm}$[16]. The beam traveling orthogonal to the elongated direction of the BEC was spatially dithered by modulating the frequency of

an acoustic-optic modulator at a few hundred kHz. This created an anharmonic, time-averaged potential. To reach the extremely cold temperatures necessary to realize long lived solitons, we evaporated to the lowest dipole trap depth in which our technical stability allowed us to realize uniform BECs.

Temperature measurement. We measured temperature below the majority atom's condensation temperature $T_c = 350\ \mathrm{nK}$ by removing the majority atoms and fitting the TOF expanded impurity atoms to a Maxwell-Boltzmann (MB) distribution[18]. Once the temperature was below T_c for the impurity atoms, MB fits systematically under estimation the temperature. Fitting the small number of impurity atoms to a Bose distribution was technically challenging due to low signal-to-noise and the addition of another free parameter, the chemical potential. To limit the number of free parameters, we preformed a global fit on the different impurity fractions where we constrain the chemical potential μ to be negative. This provided an estimate of the temperature with large uncertainties. We found for our usual operating parameters and based on information from both temperature measurements, $T = 10(5)\ \mathrm{nK}$.

Impurity characterization. We use a Blackman enveloped rf pulse at a $\sim 9\ \mathrm{G}$ magnetic field to transfer the $|F = 1, m_F = 0\rangle$ atoms primarily to the $|F = 1, m_F = +1\rangle$ internal state [29]. We varied the impurity fraction by tuning the rf amplitude. Even though the

fraction of impurity atoms before evaporation determined the fraction after evaporation, they were not equal due to more effective evaporation of the minority spin state[18]. We characterized the impurity fraction through careful, calibrated absorption imaging with a Stern-Gerlach technique during TOF to measure the relative fraction of the impurity atoms after evaporation.

Soliton creation. We applied a phase shift to half of a condensate by imaging a back-lit, carefully-focused razor edge with light red detuned by $\approx 6.8\ \mathrm{GHz}$ from the D_2 transition for $20\ \mu\mathrm{s}$.

Scattering theory of impurities. Minimizing Eq. (4) with respect to φ^*, ψ^* gives the coupled equations of motion

$$i\hbar\partial_t\varphi(z,t) = -\frac{\hbar^2}{2m_{\mathrm{Rb}}}\partial_z^2\varphi(z,t) + g|\varphi|^2\varphi + \frac{g'}{2}|\psi|^2\varphi, \tag{8}$$

$$i\hbar\partial_t\psi(z,t) = -\frac{\hbar^2}{2m_{\mathrm{Rb}}}\partial_z^2\psi(z,t) + \frac{g'}{2}|\varphi|^2\psi. \tag{9}$$

In the experiment, we observed that the soliton remained stable for long times in the presence of impurities. Therefore we neglect the last term of Eq. (8), giving the well known solitonic solution in Eq. (1) of the main text. We seek a solution for the impurity wavefunction $\psi(z)$ in the soliton rest frame. In the radial direction the single particle wavefunctions are the usual Bessel functions for a particle in a cylindrical well. For $\psi(z)$ we combine Eq. (1) and Eq. (9) with $\psi(z,t) = e^{iEt/\hbar}e^{im_{\mathrm{Rb}}v_s z/\hbar}\psi(z)$. This gives a Schrödinger equation

with a Pöschl-Teller potential[23,25],

$$\frac{\partial^2\psi(z')}{\partial z'^2} + \left[\frac{\gamma_s^2\lambda(\lambda-1)}{\cosh^2(\gamma_s z')} + k_z^2\right]\psi(z') = 0. \tag{10}$$

The dimensionless parameters are $z' = (z - v_s t)/\sqrt{2}\xi$, $k_z^2 = 4m_{\rm Rb}\xi^2/\hbar^2\,(E_z + m_{\rm Rb}v_s^2/2 - g'\rho_0/2)$, $\lambda(\lambda-1) = 2m_{\rm Rb}\xi^2 g'\rho_0/\hbar^2 = g'/g$, and $\gamma_s = \sqrt{1-(v_s/c)^2}$. g and g' are the effective 1-D interaction parameters after integrating over the transverse degrees of freedom in ψ and φ. Since the transverse wavefunctions are different, in general $g'/g \lesssim 1$. However, $R(k_z)$ is periodic in g'/g (through λ) and small variations in this parameter do not strongly affect the result. Solving for $\psi(z')$ and the scattering matrix then gives $R(k_z)$ Eq. (5) of the main text. For $\lambda \approx 1.5$, this potential also has a single, shallow bound state. Occupation of the bound state by an impurity atom can only occur through 3 body collisions (two impurity atoms and soliton), scenarios which we do not consider here.

Kinetic theory of the soliton. We define a kinetic equation with a small force $\mathbf{F}$ due to elastic collisions with lighter impurity atoms. Under this assumption the soliton distribution function $f(z,p,t)$ obeys [26]

$$\frac{\partial f}{\partial t} + \frac{\partial f}{\partial p}\mathbf{F} = \mathcal{I}\left[p,f\right] \;\; ; \;\; \mathcal{I}\left[p,f\right] = B\frac{\partial}{\partial p}\left(\frac{p}{m_s k_B T}f + \frac{\partial f}{\partial p}\right), \tag{11}$$

where $\mathcal{I}$ is the collision integral, in Fokker-Planck form. We seek a solution of the form $f = f_0 + \delta f$ where f_0 is the Maxwell-Boltzmann distribution in equilibrium, giving $\partial f_0/\partial t = \mathcal{I}\left[p, f_0\right] = 0$. From this new distribution function f, we compute $\bar{v} = b\mathbf{F}$

and find the mobility $b = k_{\rm B}T/B$, where B is the transport coefficient given in Eq. (7). Diffusion in real space is then given by $D = (k_{\rm B}T)^2/B$.

1. Scott Russel, J. Report on Waves. 311–390 and 11 plates (14th Meeting of the British Association for the Advancement of Science, York, 1844).

2. Ostrovsky, L. A. & Stepanyants, Y. A. Do internal solitions exist in the ocean? *Reviews of Geophysics* **27**, 293–310 (1989).

3. Drummond, P. D., Shelby, R. M., Fiberg, S. R. & Yamamoto, Y. Quantum solitons in optical fibres. *Nature* **365**, 307 (1993).

4. Burger, S., Bongs, K., Dettmer, S., Ertmer, W. & Sengstock, K. Dark Solitons in Bose-Einstein Condensates. *Physical Review Letters83* **83**, 5198–5201 (1999).

5. Einstein, A. On the Movement of Small Particles Suspended in Stationary Liquids Required by the Molecular-Kinetic Theory of Heat. *Annalen der Physik* **17**, 549–560 (1905).

6. Dauxois, T. & Peyrard, M. *Physics of Solitons* (Cambridge University Press, Cambridge, UK, 2006).

7. Agrawal, G. Nonlinear fiber optics: its history and recent progress. *J. Opt. Soc. Am. B* **28**, 0–1 (2011).

8. Strecker, K. E., Partridge, G. B., Truscott, A. G. & Hulet, R. G. Formation and propagation of matter-wave soliton trains. *Nature* **417**, 150–153 (2002).

9. Denschlag, J. Generating Solitons by Phase Engineering of a Bose-Einstein Condensate. *Science* **287**, 97–101 (2000).

10. Muryshev, a., Shlyapnikov, G. V., Ertmer, W., Sengstock, K. & Lewenstein, M. Dynamics of Dark Solitons in Elongated Bose-Einstein Condensates. *Physical Review Letters* **89**, 110401 (2002).

11. Becker, C. *et al.* Oscillations and interactions of dark and dark-bright solitons in Bose-Einstein condensates. *Nature Physics* **4**, 9 (2008).

12. Weller, A. *et al.* Experimental Observation of Oscillating and Interacting Matter Wave Dark Solitons. *Physical Review Letters* **101**, 1–4 (2008).

13. Hasegawa, A. & Matsumoto, M. *Optical solitons in fibers*, vol. 2 (Springer-Verlag, Heidelberg, 2003), third edn.

14. Anderson, B. P. *et al.* Watching dark solitons decay into vortex rings in a Bose-Einstein condensate. *Physical Review Letters* **86**, 2926–2929 (2001).

15. Ku, M. J. H. *et al.* Motion of a solitonic vortex in the BEC-BCS crossover. *Physical Review Letters* **113**, 1–5 (2014).

16. Lin, Y.-J. J., Perry, A. R., Compton, R. L., Spielman, I. B. & Porto, J. V. Rapid production of 87Rb Bose-Einstein condensates in a combined magnetic and optical potential. *Physical Review A - Atomic, Molecular, and Optical Physics* **79**, 1–8 (2009).

17. Fang, F., Olf, R., Wu, S., Kadau, H. & Stamper-Kurn, D. M. Condensing magnons in a degenerate ferromagnetic spinor Bose gas. *Phys. Rev. Lett.* **116**, 095301 (2016).

18. Olf, R., Fang, F., Marti, G. E., MacRae, A. & Stamper-Kurn, D. M. Thermometry and cooling of a Bose-Einstein condensate to 0.02 times the critical temperature. *Nature Physics* **11**, 06196 (2015).

19. Mateo, A. M. & Brand, J. Stability and dispersion relations of three-dimensional solitary waves in trapped Bose-Einstein condensates. *New Journal of Physics* **17**, 125013 (2015).

20. Zaremba, E. Sound propagation in a cylindrical Bose-condensed gas. *Phys. Rev. A* **57**, 57 (1998).

21. Parker, N. G., Proukakis, N. P. & Adams, C. S. Dark soliton decay due to trap anharmonicity in atomic Bose-Einstein condensates. *Physical Review A - Atomic, Molecular, and Optical Physics* **81**, 1–10 (2010).

22. Cockburn, S. P. *et al.* Fluctuating and dissipative dynamics of dark solitons in quasi-condensates. *Physical Review A* **84**, 43640 (2011).

23. Pöschl, G. & Teller, E. Bemerkungen zur Quantenmechanik des anharmonischen Oszillators. *Zeitschrift für Physik* **83**, 143–151 (1933).

24. Cooper, F., Khare, A. & Sukhatme, U. Supersymmetry and quantum mechanics. *Physics Reports* **251**, 267–385 (1995).

25. Çevik, D., Gadella, M., Kuru, S. & Negro, J. Resonances and Antibound states for the Pöschl Teller Potential: Ladder operators and SUSY partners. *Physics Letters A* **380**, 1600–1609 (2016).

26. Lifschitz, E. & Pitaevskii, L. *Physical kinetics* (1983).

27. Fedichev, P. O., Muryshev, A. E. & Shlyapnikov, G. V. Dissipative dynamics of a kink state in a Bose-condensed gas. *Phys. Rev. A* **60**, 3220 (1999).

28. Efimkin, D. K., Hofmann, J. & Galitski, V. Non-Markovian quantum friction of bright solitons in superfluids. *Physical Review Letters* **116**, 225301 (2016).

29. Jiménez-García, K. *et al.* Phases of a two-dimensional bose gas in an optical lattice. *Physical Review Letters* **105**, 20–23 (2010).

Acknowledgements We thank Dmitry Efimkin for his extension of reference[27] giving our Eq.(7); additionally, we thank Martin Link and Stephen Eckel for carefully reading our manuscript. This work was partially supported by the ARO's Atomtronics MURI, by the AFOSR's Quantum Matter

MURI, NIST, and the NSF through the PFC at the JQI. HMH acknowledges additional fellowship support from the National Physical Science Consortium and NSA. VG acknowledges support from the Simons Foundation.

Author Contributions L.M.A. configured the apparatus for this experiment and led the data acquisition and analysis effort and the manuscript preparation. H.M.H. performed theoretical calculations and prepared the theory discussions in the manuscript. H.-I L. and D.G. contributed to all experimental aspects of this project and to the writing of the manuscript. V.G. proposed the experiment concept and contributed to the development of the theory and to the writing of the manuscript. I.B.S. wrote the author contributions.

Competing Interests The authors declare that they have no competing financial interests.

Correspondence Correspondence and requests for materials should be addressed to I.B.S. (email: ian.spielman@nist.gov).

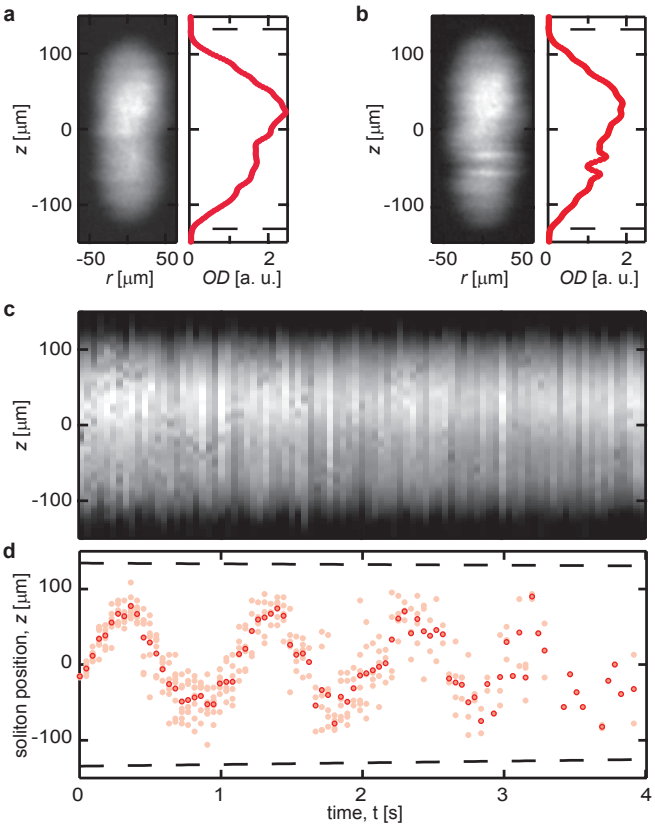

Figure 1 | Soliton oscillations. a, An absorption image after a $19.3\ \mathrm{ms}$ TOF of an elongated condensate without a soliton and a longitudinal density distribution obtained by averaging over the remaining transverse direction. **b**, An absorption image and 1-D distribution at time $t = 0.942\ \mathrm{s}$ with a soliton with $\approx 30\%$ imaged contrast. **c**, A subset of the data where each 1-D distribution is a unique realization of the experiment plotted versus time t. **d**, The axial position z_i of the soliton (light pink) versus time t for different realizations of the experiment. We repeated each measurement 8 times. Dashed lines represent the edges of the elongated condensate. The dark markers represent the average soliton position $\langle z_i \rangle$ at each time t.

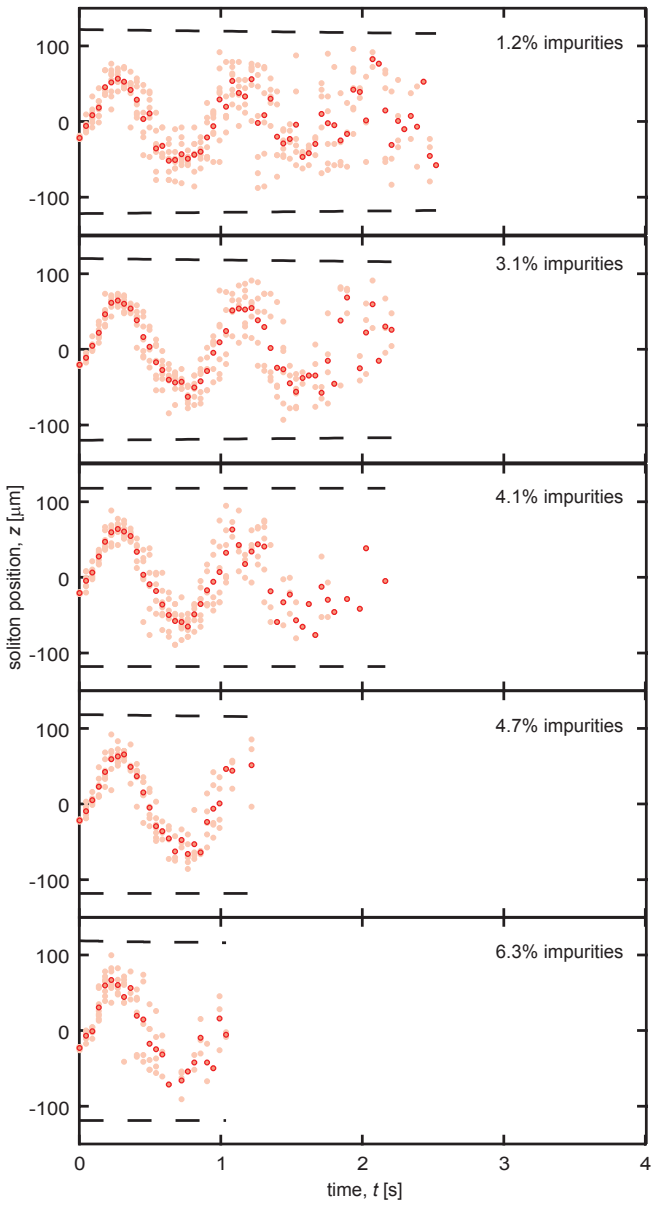

Figure 2 | Impact of impurities. Here, we plot the position z_i of the soliton (light pink) versus time t after the phase imprint for different impurity levels. The dark pink markers represent the average position $\langle z_i \rangle$ for each time t. Dashed lines represent the endpoints of the condensate versus t.

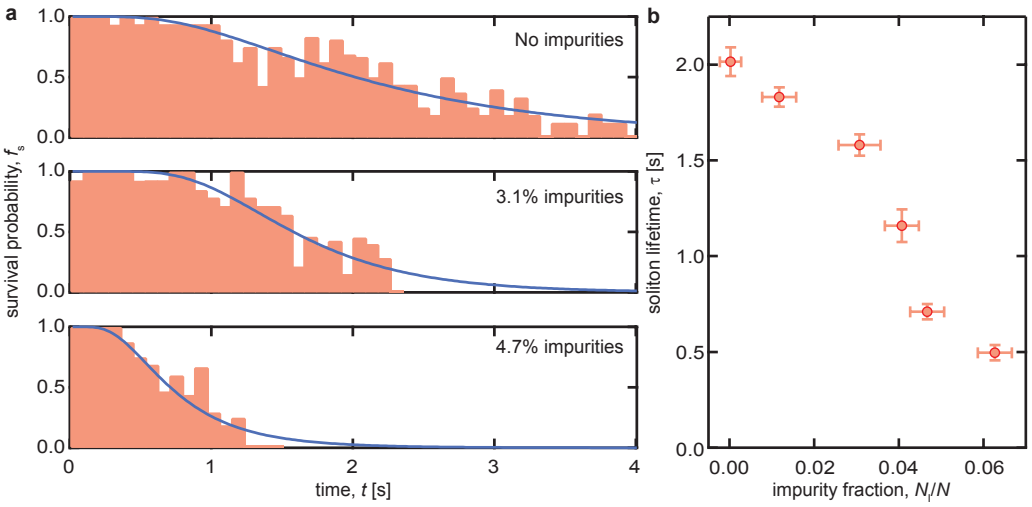

Figure 3 | Soliton lifetime in the presence of impurities. **a**, Histograms of soliton occurrence probability f_s versus time t after phase imprint. The blue solid curves are fits to the lognormal based survival function from which we extract the lifetime τ. For each impurity fraction, we stopped collecting data when f_s fell below about 0.2. **b**, Lifetime τ extracted from fit to the survival fraction f_s versus impurity fraction $N_{\rm I}/N$.

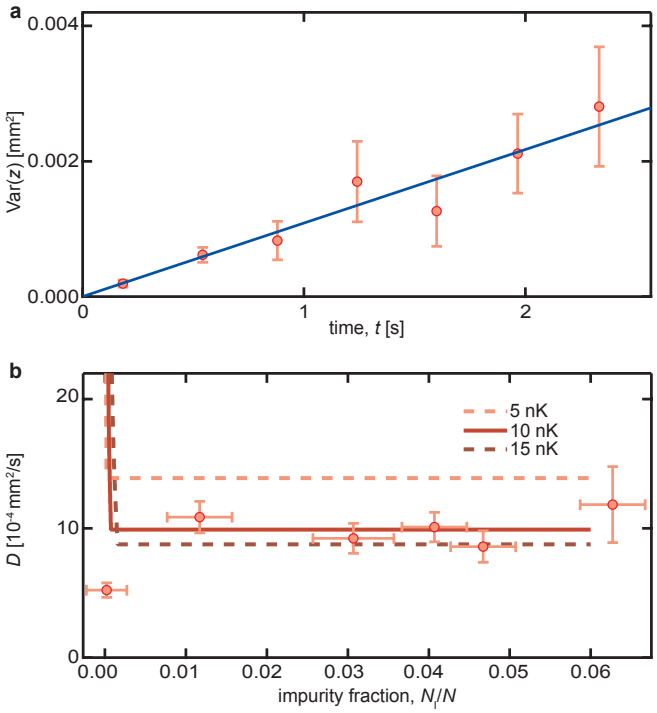

Figure 4 | Brownian diffusion constant dependence on impurities. **a**, An example for the linear fit of $\mathrm{Var}(z)$ versus t for 1.2% impurities. Data is binned into 0.36s bins, the uncertainties are the sample standard deviation. **b**, The diffusion coefficient D versus impurity fraction N_{I}/N. The experimental results (markers) are extracted from the slope of a linear fit of the sample variance $\mathrm{Var}(z)$ versus time t. The uncertainty in D is the uncertainty from that fit. See methods for explanation of uncertainty in N_{I}/N. The theory curves (solid and dashed curves) plot the calculated D for our measured temperature.